Journal of Environmental Chemical Engineering 9 (2021) 105556

Contents lists available at ScienceDirect

Journal of Environmental Chemical Engineering

journal homepage: www.elsevier.com/locate/jece

Improving the discharge of capacitive granules in a moving bed reactor

C. Borsje [a,b], T. Sleutels [b], C.J.N. Buisman [a,b], A. ter Heijne [a,*]

[a] Wetsus, European Centre of Excellence for Sustainable Water Technology, P.O. Box 1113, 8900 CC Leeuwarden, Netherlands
[b] Environmental Technology, Wageningen University, P.O. Box 17, 6700 AA Wageningen, Netherlands

ARTICLE INFO

Editor: Dr. GL Dotto

Keywords:
MFC
BES
Capacitor
Bioanode

ABSTRACT

Bioanodes can be used to recover the energy and nutrients from wastewater in bioelectrochemical systems. The use of capacitive electrodes can improve the current density produced by these bioanodes. Moving bed reactors are studied to produce high current densities, by using capacitive granules for charge storage and with a high bioanode surface area. The bioanodes store charge in the granules, which are intermittently discharged at a current collector. In principle, this allows for more current density in the electrochemical cell, because both faradaic and capacitive currents are harvested. One of the limiting factors of this technology is the capacitive discharge rate. In abiotic tests, the capacitive discharging was most improved by changes in potential difference between the current collector and charged granules (ΔE 0.3 and 0.5 V). Increasing the bulk electrolyte conductivity also increased the transferred charge, which could originate from the increased capacitance – as measured in a separate setup. Discharging from both sides of the granular bed, as compared to discharging from one side, reduced the maximum distance to the current collector, which increased the transferred charge, irrespective of an increase in bulk electrolyte conductivity. This showed the electrical resistance was more important in determining the transferred charge than the ionic resistance. Further analysis of the discharging process showed that discharging increased the local conductivity through the release of ions from the granules. This offers opportunities for the treatment of low conductivity wastewaters. These results provide new insights to further improve capacitive bioanodes.

1. Introduction

Recovery of energy and nutrients from waste streams is a necessity for a sustainable society. Municipal wastewater alone contains considerable amounts of nitrogen (14%), phosphorus (7%) and potassium (19%) required in agriculture [1]. Globally, wastewater contains enough energy to provide electrical power to 158 million households [1]. Bioelectrochemical systems (BESs) can be used to recover the energy and nutrients from wastewater [2]. An electrical current can be generated by electroactive bacteria growing on the anode of BESs. These bacteria oxidize dissolved organics in wastewater and release electrons to the electrode. The current can be used to generate electrical power in Microbial Fuel Cells [3] or produce H_2 [4,5], NaOH [5,6], H_2O_2 [7] or separate NH_3 [8–10], PO_4^{3-} [11,12] and NaCl [13] from wastewater. Low current densities have thus far limited the implementation of BESs [14,15]. Capacitive bioanodes have been shown to produce more charge than non-capacitive bioanodes by using intermittent charging and discharging [16,17]. Capacitive bioanodes are a special configuration of BESs, that use capacitive electrodes, which can store and release charge [18] in the pores of activated carbon [19]. The charge, stored during charging by the electroactive bacteria, is released as a capacitive current during discharging. This capacitive current is produced on top of the faradaic current produced directly by the bioanode [16]. The charge is stored by the formation of an electrical double layer: electrons are stored at the surface of the pores [18], and cations from the electrolyte are attracted, or anions are expelled, to balance the negative charge [20]. These cations are released during discharging, which is expected to increase the local conductivity of the electrolyte [15].

To be able to use large amounts of activated carbon granules, and thus a large specific surface area of electrode surface, as capacitive bioanodes, fluidized bed bioanode reactors have been developed [15,21–30]. The granules function as charge carrier as well as biofilm carrier, and are discharged at a current collector to produce a continuous current [22]. These granules are fluidized to make intermittent contact with a current collector, by stirring [21,23], liquid [23–29] and gas [15,22,30]. The reactors make use of intermittent charge storage of the

* Correspondence to: P.O. box 17, 6700 AA Wageningen, Netherlands.
E-mail address: annemiek.terheijne@wur.nl (A. ter Heijne).

https://doi.org/10.1016/j.jece.2021.105556
Received 17 February 2021; Received in revised form 17 April 2021; Accepted 19 April 2021
Available online 24 April 2021

capacitive bioanode granules by using the large ratio of external surface area per volume of granules for the biofilm to produce charge. The stored charge is then harvested by discharging to a relatively small surface area electrode [30], which is the most expensive part of a bio-electrochemical system [31]. Thus, the costs per active volume of reactor are decreased. The current produced in these type of reactors, however, is still several orders of magnitudes lower (257 $A/m^3_{granules}$) [30] than the maximum current that could be achieved when a single granule is used as bioanode (76.8×10^3 $A/m^3_{granule}$) [32]. To fully utilize the capabilities of capacitive bioanodes, the stored charge should be recovered using a high discharge current, consisting mainly of a capacitive current [22]. This will allow for the conversion of a high organic loading and to recover a high volumetric current. Studying the capacitive current is less difficult under abiotic conditions as the biofilm affects both the charging and discharging processes [33].

In a moving bed reactor, the granules move as a moving granular bed through an internal discharge cell, using a gas lift to fluidize and transport the granules back to the top of the reactor [22,30,34]. To increase the volumetric current from this moving capacitive bed, a better understanding of the discharging process of the granules is required. Figure 1 shows four factors influencing the capacitive discharge in the moving bed. The discharge rate is determined by the potential difference between the charged granules and current collector [19,22,30]. Both the capacitance and the resistance over the granular bed affect the potential difference between the granules and current collector [35,36]. For a bed of capacitive granules this resistance consists of: contact between the granules, between the granules and the current collector, the resistance of the granular material itself [37] and the resistance of the electrolyte. The conductivity of the electrolyte also affects the capacitance of the granules.

The residence time in the discharge cell is determined by the granule flowrate, which in turn affects the time the granules are in contact with the current collector [22,30]. The residence time therefore affects how much charge is transferred per granule, when it is in the discharge cell.

The aim of this study therefore is to optimize process parameters for discharge of capacitive granules under abiotic conditions. We investigated the discharging of charged granules as a function of 1) the potential difference between current collector and granules 2) the conductivity of the bulk electrolyte, 3) the distance between granules and current collector, 4) the flowrate of the granular bed.

2. Materials and methods

2.1. Moving bed reactor

The moving bed reactor was constructed similar to the gas lift reactor in our previous study [22]. The granules were recirculated in the reactor, using a gas lift, which consisted of a top and bottom glass volume, with a polymethylmethacrylate (PMMA) electrochemical cell attached in between. The granules were transported from the bottom to the top of the reactor by the gas lift. From the top, the granules settled down on top of the granular bed slightly above the electrochemical cell. The granules moved as a bed through the cell and back into the bottom part of the reactor. The electrochemical cell was used to charge and discharge the capacitive granules as they moved through the cell.

The N_2 flow for the gas lift was controlled using a mass flow controller (Mass-stream D-6311 with ± 1% accuracy, Bronkhorst Nederland B.V., Veenendaal, Netherlands). The gas flow was adjusted to change the granular flowrate, which was used as one of the experimental variables (see Sections 2.2. and 2.4). The reactor volume in which the granules circulated was 1.2 L. The electrolyte recirculated at 80 mL/min via a recirculation bottle with 0.3 L liquid volume, where the gas effluent from the gas lift was sparged through and separated from the electrolyte. This ensured an anaerobic environment. The counter electrode had a volume of 2.3 L, including the flow compartments in the electrochemical cell and the recirculation bottle, through which the electrolyte was recirculated at 80 mL/min.

The electrochemical cell, also called the discharge cell, was constructed with two pairs of working electrodes and counter electrodes (Fig. 2), to be able to connect the granule bed to the working electrode on both sides. The electrodes consisted of titanium with a mesh insert coated with Pt/Ir (Magneto Special Anodes B.V., Schiedam, Netherlands). The electrodes were separated by a cation exchange membrane (Ralex CMH-PP, Mega c.z., Stráž pod Ralskem, Czech Republic). The working electrodes were separated by 10 mm thick transparent PMMA pieces. Since the flow channel had a projected surface area of 22.3 cm^2, both the exposed membrane area and the area enclosed by the mesh insert, in the electrodes, were 22.3 cm^2. The 10 mm separation created a space for the moving bed of granules. A capillary, attached to a 3 M KCl salt bridge and an Ag/AgCl reference electrode, was inserted in the cell between the working electrodes.

A Pt/Ir wire (80:20 w%, 0.25 mm, Advent-RM, Oxford, United Kingdom), of which approximately 1 cm was exposed to the solution and granules, was placed in the granular bed above the electrochemical cell, to measure the potential of the granules against a locally placed reference electrode, before they were charged or discharged. The granular material (bulk density 0.486 g/cm^3, coconut based HR5, Eurocarb) was sieved between 0.5 and 0.8 mm (stainless steel sieves, VWR). The system was filled with 176 g of granules (weight after washing and overnight drying at 105 °C).

The electrolytes were prepared from demineralized water and Na_2SO_4, under constant mixing, until the conductivity reached 5.5 and 15 mS/cm (pH/Cond 340i, WTW, Weilheim, Germany). Na_2SO_4 was chosen to avoid unwanted electrochemical reactions such as chlorine

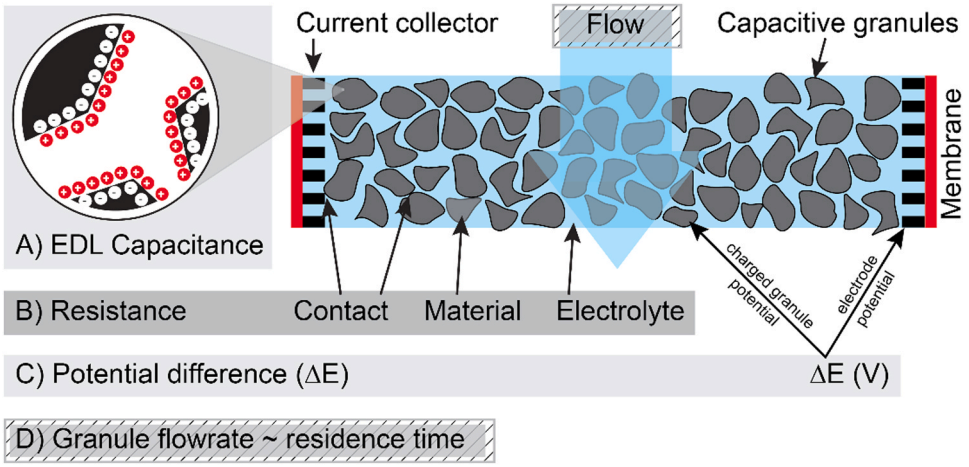

Fig. 1. Factors influencing the capacitive discharge from a moving bed electrode. The capacitance is formed by the electrical double layer (EDL) on the surface of the porosity. The resistance of the granular bed consists of contact resistance, material resistance of the granules and the ionic resistance of the electrolyte. The potential difference (ΔE) is the difference between the electrode potential and the potential of the charged granules. The flowrate of the granules through the cell influences the residence time of the granules in the discharge cell.

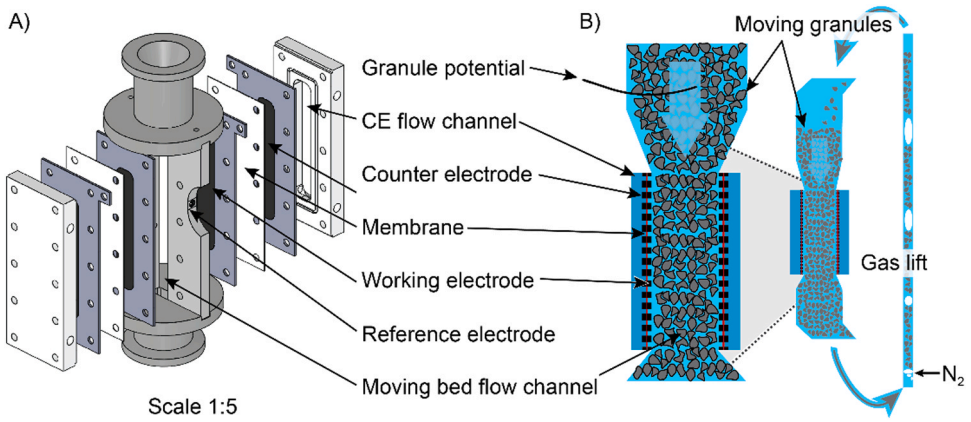

Fig. 2. A) A Computer Assisted Design (CAD) drawing of the electrochemical cell, with vertical cross sections. B) A schematic view of the cell, perpendicular to the electrode surfaces showing the 10 mm separation between the working electrodes, and its position in the gas lift reactor (Modified from Ref. [22]).

formation [38]. The electrolyte was chosen as a simple salt solution to avoid introducing extraneous variables that may arise from the complex composition of (synthetic) wastewater. The 5.5 mS/cm solution was chosen to match the conductivity of the synthetic medium used previously [30], and was increased to study the effect of higher bulk electrolyte conductivity. The same solutions were used as electrolyte in the capacitance measurements. The electrolyte for the counter electrode was a 50 mS/cm Na_2SO_4 solution. The concentration of the electrolytes was 25 mM (for 5.5 mS/cm), 107 mM (for 15 mS/cm), and 412 mM (for 50 mS/cm), calculated using the tabular data in Section S3 of the Supporting information. The influent for the reactor was constantly flushed with N_2, and the recirculation vessel was flushed with N_2 as well. The influent electrolyte solutions were pumped into the reactor at 1.3 mL/min.

2.2. Experimental strategy

The performance of the moving bed was determined from the charge transferred during discharging. The granules were first charged at − 0.5 V vs Ag/AgCl, until they reached about − 0.49 V vs Ag/AgCl, which is close to the (open circuit) potential of acetate oxidation by bioanodes [39]. The discharging was studied for four different factors (Table 1): A) discharge potential, leading to a potential difference with the charged granules, B) bulk electrolyte conductivity, C) 1 or 2 working electrodes (WE), reducing the maximum distance between granules and current collector by a factor of two, and D) low and high flowrate of the moving granular bed.

The concentration of the bulk electrolyte affects the capacitance of the granules [35]. This means more charge can be stored and discharged for the same potential difference. Therefore, the capacitance of the granules was studied in the same electrolyte as used in the moving bed experiments.

2.3. Electrochemical measurements and control

The electrochemical cells were controlled by potentiostats (nStat, Ivium Technologies B.V., Eindhoven, Netherlands), with the working electrodes controlled against Ag/AgCl/3 M KCl reference electrodes (+203 mV vs standard hydrogen electrode (SHE), QM711X/Gel, ProSense, Oosterhout, Netherlands). All further potentials are referenced to the Ag/AgCl reference electrode.

The reference electrodes were attached to 3 M KCl salt bridges and capillaries (4 mm diameter, Prosense, Oosterhout, Netherlands). One potentiostat was used to control either one or both working electrodes, together with the matching counter electrodes, against the reference electrode. Another potentiostat was used to measure the potential of the second working electrode and the potential of the granules. The channels were synchronized and set to floating mode (measured against common ground) using Iviumsoft (Iviumsoft version 4.946, Ivium Technologies B.V., Netherlands).

The granules were charged during initial experiments. Before the start of the experiments in Table 1, the granules had a potential of − 0.47 V. Each discharge experiment had four phases: 1) pre-charging, 2) self-discharge monitoring, 3) discharging and charging cycles, 4) charging after. In the pre-charging phase, the granules were charged for 12 cycles of 50 min at − 0.5 V, followed by 10 min open circuit (OC): this allowed for fully charging and monitoring of the intermediate charging process (at OC). The pre-charging was followed by 2 h of OC to monitor the self-discharge process (for example parasitic faradaic processes such as oxygen reduction, from oxygen crossover from the counter electrode over the membrane) [40]. After pre-charging, the experiment was performed by discharging and charging the granules for 10 sequential cycles. Discharging was done at − 0.2 V and 0 V, for 20 min (long discharging) (or short discharging using 5 min, see Supporting Information S2), and followed by 1 h of charging at − 0.5 V, for

Table 1
Overview of performed experiments.

Charge – discharge cycle (working electrode potential)	Cell configuration (# working electrodes)	Electrolyte conductivity	Flowrate	Discharge time	Figure #
Charging − 0.5 V Discharging − 0.2; 0 V	2WE	Low & High	Low	Long	3
Charging − 0.5 V Discharging 0 V	1WE and 2WE	Low & High	Low	Long	4
Residence time Charging − 0.5 V Discharging 0 V	2WE	High	Low & High	Long	5

a cycle of 1 h and 20 min. The difference in potential between the charged granules and the current collector thus became about 0.3 and 0.5 V. After the cycles, the next experiment was prepared for by charging the granular bed again for 6 cycles of − 0.5 V for 50 min and 10 min of OC. The whole program was run 3 times, to obtain 30 cycles of discharging and charging.

The cumulative charge, calculated by Iviumsoft from the current over time, was used to differentially determine the charge per discharge cycle. The potential difference (ΔE) for each cycle was calculated by subtracting the measured potential of the granules, at the start of the cycle, from the working electrode potential. The resistance during discharging was calculated by dividing the ΔE by the current. The average resistance and associated standard deviation were calculated for each cycle.

Since discharging of electrons leads to release of ions, both from the charge stored in the electrical double layers, we estimated the increase in conductivity as a result of discharge. The ions released during the discharging were calculated by multiplying the charge, from the current, with 1.04×10^{-5} mol/Coulomb Na^+ (as $Q/(n \times F)$, with $n = 1$ and $F = 96485$ C/mol e^-). The ions were released into the electrolyte in the discharge cell with a volume of 1–bulk density of granules, or 0.514 mL electrolyte per mL discharge cell, during the discharge time. The concentration of released ions, that adds to the bulk concentration, was calculated by multiplying the concentration of ions released per second by the residence time in the discharge cell (see Table 2). The concentration of Na^+-ions released was converted to a Na_2SO_4 solution, which assumed SO_4^{2-} as the counter ion in the local solution. The solution conductivity was determined by using regression on reported concentration to conductivity values for a Na_2SO_4 solution. The concentration to conductivity values were calculated by methodology described in Ref. [41] for concentrations below 56 mM [41], and regression on concentration to conductivity values from tabular data [42] for concentrations above 56 mM. See Supporting information S3 for the data and regression results.

The ohmic resistance over the granular bed was measured as the real component of high frequency impedance scans (PGSTAT302N with FRA32M, Metrohm Autolab, Utrecht, Netherlands) at constant current (5 kHz, 0 ± 1 mA, 100 repetitions) between the two working electrodes, with a 5-min OC period before the impedance scans. The impedance scans were performed in between the discharging experiments. The resistance of the granular bed was determined using the cell constant, which was determined as 0.045 1/cm by multiplying the ohmic resistance of the cell in an electrolyte with an known conductivity (no granules) [43]. The ohmic resistance was measured together with the bulk electrolyte solution. A linear regression analysis (see Supporting information S4 for the data and regression results) was used to determine the ohmic resistance for each experiment, as the bulk conductivity varied slightly for each experiment. The ohmic resistance was further adapted to match the cell configuration: for the 2WE configuration, the ohmic resistance was assumed to be over half of the width of the granular bed (5 mm), as compared to ohmic resistance for the 1WE configuration, which was over the full width of the granular bed (10 mm).

Measurements of granule capacitance were performed on small volumes of granules (9–20 mg) in an electrochemical cell developed in a previous study [30], where the granules were pressed against the working electrode. The counter electrode was Pt/Ir wire. The reference electrode was placed directly in the electrolyte. The electrolyte was flushed constantly with N_2 under constant stirring.

Table 2
The residence time and recirculation time of the granular bed resulting from the low and high granule flowrate experiments.

	Residence time cell (s)	Circulation time (s)
Low flowrate	194 ± 23	3186 ± 386
High flowrate	67 ± 17	1096 ± 272

The capacitance was measured by charging first in cycles of − 0.5 V and OC, until the OC potential was lower than − 0.45 V. The granules were then sequentially discharged and charged at 20 μA and − 20 μA respectively, for 10,000 s each, until the potential was 0 V. The measurement was repeated until at least 7 discharge cycles were available for analysis. During discharging, the potential first quickly increased due to the ohmic drop (iR) and then increased linearly as the capacitance discharged [18,44]. To determine the capacitance of the sample of granules, the current (C/s) was divided by the slope of the potential during discharging (V/s), which was determined from linear regression analysis [45]. The capacitance was then normalized to the weight of the sample of granules (washed 3 times in ultrapure water and dried overnight at 105 °C).

2.4. Granule flowrate

The flowrate of the granules moving through the electrochemical cell was determined from videos (1080p, 60 fps, Nikon D750 with Sigma 105 mm macrolens at f/11) taken through the transparent sides of the cell. The focus area was illuminated [22]. The videos were analyzed using Fiji [46] ImageJ2 [47]. The granular flow velocity was determined 10 times per video, by measuring the distance travelled and dividing it by the time between the first and last frame for the granule. The residence time in the discharge cell (volume 22 mL) was calculated by dividing the 11 cm length, over which the membrane was exposed, by the granular flow velocity. The circulation time, which includes the residence time, was calculated by dividing the total granule volume (362 mL) by the granular flow velocity, multiplied by the horizontal cross section of the cell: 2 cm^2. See Supporting information Fig. S1 for an example of the measurement. During the experiments, the flow of the granular bed was changed by controlling the gas flow in the gas lift: an increase in gas flow from 140 to 200 mL/min of N_2 resulted in a 2.9 times higher granular flow of the granular bed in the discharge cell: Table 2 shows the average and standard deviations for the residence time and recirculation time at the low and high flowrate.

3. Results and discussion

3.1. Charge transfer increased with higher potential difference and with higher electrolyte conductivity

First, we studied how total charge transferred from granules to current collector was affected by the potential difference (ΔE) between the current collector and the charged granules, and by solution conductivity. The granules were pre-charged at − 0.5 V and then subjected to discharge – charge regimes, in which they were discharged for 20 min and charged at − 0.5 V for 60 min, for a total of 30 cycles. The granules were discharged at − 0.2 V and 0 V, which resulted in a ΔE of about 0.3 and 0.5 V. In Fig. 3, the produced charge during discharging, in both low and high conductivity electrolyte, is shown against the measured ΔE. The current decreased from a peak to a stable current, with on average (for all experiments in Table 1) 88% of the recovered charge produced from the average current over the last 10 min of discharging. The transferred charge increased as expected at higher ΔE. At low conductivity, the charge increased 2.5 times from 175 C to 429 C when ΔE was increased from 0.3 to 0.5 V. At high conductivity, the charge increased 2.0 times from 257 C to 507 C when ΔE was increased from 0.3 to 0.5 V. The higher ΔE increased the transferred charge on average 2.3 times, which was not proportional to the increase in ΔE (on average 1.6 times). This is likely related to the total resistance during discharging, which we will discuss later (see Section 3.4).

The bulk conductivity was increased from 6 mS/cm to 16 mS/cm, thereby reducing the ionic resistance of the electrolyte. With the change to high conductivity electrolyte, the ohmic resistance decreased from 0.70 ± 0.02 Ω to 0.32 ± 0.02 Ω. The change in ohmic resistance (2.3 times) was thus very close to the change in electrolyte conductivity (2.5

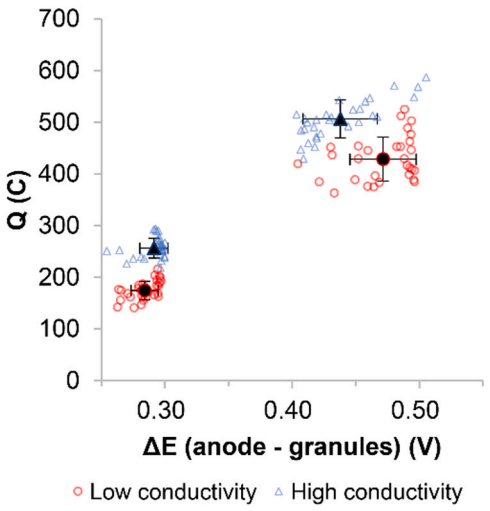

Fig. 3. Charge from granules discharged at different applied ΔE (0.3 V and 0.5 V) and at low and high conductivity (6 and 16 mS/cm). The black filled markers are the average values. The error bars show the standard deviation of the produced charge and the measured ΔE.

times). The discharge experiments in Fig. 3 show that at high bulk electrolyte conductivity, the average discharge was 1.5 times higher compared to at low conductivity, at a potential difference of 0.3 V, and 1.2 times higher for discharging at a potential difference of 0.5 V. Therefore, the increase in bulk electrolyte conductivity resulted in more transferred charge, which was however, not proportional to the increase in electrolyte conductivity or the decrease in ohmic resistance over the granular bed (see Section 3.4.).

Aside from the bulk electrolyte, the electrolyte in the pores of the granules was also affected by changing from low to high conductivity, which affects the formation of electrical double layers that form the capacitance [48]. The capacitance of the granules was measured by charge – discharge experiments on small volumes of granules in a separate test cell, in the two electrolytes. There was an effect of the bulk electrolyte conductivity on the capacitance of the granules: the gravimetric capacitance increased from 75 ± 18 F/g to 104 ± 11 F/g. This increase is in line with the findings of Zhao and colleagues, where the capacitance was reduced at low molarity compared to high molarity NaCl solution [48]. The increased capacitance could be one of the reasons for the increased charge in the higher concentrated electrolyte and may result from the lower ion transport resistance in the porosity.

In most experiments, the measured ΔE differed slightly from the applied ΔE. This was caused by less efficient charging than discharging. As the granules were discharged, the granule potential increased. Especially at the high applied ΔE and high conductivity electrolyte, when more charge was transferred, the granule potential increased more during discharge than it decreased during charge, resulting in a lower measured ΔE than applied ΔE. To see if this shift in ΔE was indeed due to a difference in charging and discharging, the effect of discharging and charging time was studied further, by applying cycles with a shorter discharge time of 5 min, compared to the 20 min used in the other experiments, while charging time was unchanged. The results, shown in the Supplementary information Fig. S2, show that in this case, the measured ΔE indeed stayed closer to the applied ΔE, meaning that charge and discharge were more in balance. The short discharge period removes less total charge from the granules than the longer discharge period, which means the ΔE changes less. The higher ΔE is a higher driving force for the discharge current, and thus results in a higher current density, though the charge recovered is less due to the shorter discharge period.

3.2. Charge transfer increased when the bed was discharged on both sides

To study if the transferred charge was affected by electrical resistance or by ionic resistance in the granular bed, the granules were discharged at 1 or 2 WEs, in low and high conductivity electrolyte at a ΔE of 0.5 V. We previously showed that discharging with the electrode closest to the membrane was more efficient than an electrode on the other side of the granular bed [22]. For this study, the electrochemical cell was built using WEs on both sides of the granular bed, that had a thickness of 10 mm, together with a membrane and counter electrode on both outer sides of the system. Using both WEs, instead of one WE, reduced the maximum distance from the granules to the current collector by a factor 2, and thus reduced both electrical and ionic resistance by a factor 2. Aside from the distance, the second working electrode also provided additional surface area (also doubling the surface area of the membrane and cathode). Fig. 4 shows the charge from discharging at 1 and 2 working electrodes, in the two electrolytes, for all cycles and the average per experiment. With the additional current collector, the transferred charge increased: in the high conductivity electrolyte, the average charge increased from 270 C to 507 C, and in low conductivity the average charge increased from 199 C to 429 C. Thus, by discharging on both sides of the granular bed the transferred charge increased on average 2.1 times. As discussed earlier (Section 3.1), due to the less efficient charging than discharging, the ΔE showed a larger variation for more charge recovered during discharging. During these experiments, the change from low to high salinity resulted on average in 1.3 times higher charge. From this we conclude that the effect of the bulk electrolyte conductivity on the average charge was less pronounced than the increase in charge from using an additional current collector, and therefore that the electrical resistance is more important in determining the transferred charge during discharging than the ionic resistance.

In suspension flow capacitive deionization (FCDI) systems, where an activated carbon powder slurry is charged in an electrochemical cell to desalinate the feed stream [36,44,49–64], higher carbon content was used to decrease the electrical resistance [55,65]. By simultaneously varying the salt concentration, it was found that the voltage drop was reduced by 72% by the higher carbon content, in contrast to 36% due to increased electrolyte conductivity [65]. Thus, the electrical resistance is more important than ionic resistance for the performance of FCDI systems. These results support our conclusions.

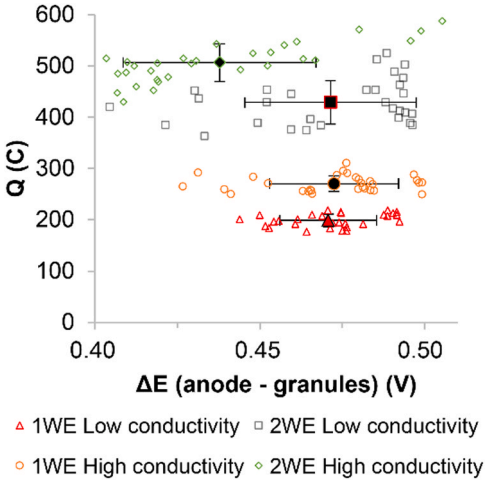

Fig. 4. The charge from granules, discharged at 1 or 2 working electrodes (WEs), versus measured ΔE. The black filled markers are the average values, and the error bars show the standard deviation.

3.3. Charge transfer increased at higher flowrate

To study the effect of the residence time in the discharge cell, the flowrate of the granules was varied. The residence time determined the time for discharging the granules that passed through the discharge cell in the 20 min of discharging (in the charge and discharge cycles). Through the circulation speed of the granules via the gas lift, the residence time of the granules in the discharge cell changed. At high flow rate the residence time was 67 s, with a circulation time of 18 min, compared to 194 s, with a circulation time of 53 min, at low flow rate (see Table 2). Fig. 5 shows that with a shorter residence time, 1.3 times more charge was produced, than with a longer residence time.

On the level of singular granules, the capacitive current decreases the longer a granule is discharged, which increases the potential of the granule [19,32]. For the moving bed reactor this effect can be translated to the granules in the discharge cell: as the granules were discharged in the discharge cell, the potential of the granules increased, decreasing the ΔE. We can therefore assume the ΔE decreased over the length of the discharge cell. As the ΔE was the driving force for the capacitive current, there the average current over the length of the discharge cell decreased as well. As the granules resided longer in the discharge cell for the low flowrate, the ΔE and current decreased more, resulting in lower recovered charge compared to the short residence time situation.

Additionally, the difference in circulation time affected the volume of granules that could contribute to the discharge current in the 20 min of discharging. For the low flowrate, only 38% of the granules (and therefore only 38% of the potentially available charge) passed through the discharge cell in the 20 min discharging, while for the high flowrate the total granule volume passed through the discharge cell 1.1 times in the 20 min discharging. At the higher flowrate, the recovered charge in those 20 min was thus spread over more granules. This translated to a smaller change in ΔE, and therefore a higher average current over the cell.

The result of the lower gradient over the length of the cell, due to the short residence time and the larger participating volume, was a higher average current density, resulting in a higher amount of charge recovered, with a higher average ΔE, as seen in Fig. 5. For the abiotic discharging, a higher flowrate is thus preferred.

For bioanodes, high discharge current is preferred as the charge recovered is recharged in the charging phase of the circulation cycle in the moving bed [22,30], which increases the efficiency over the total reactor volume. However, at the high flowrate, there was a smaller change in potential of the granules. This may have implications for the operation of bioanodes, for which the electro-active activity depends on the potential of the electrode, in this case the potential of the granule. The competition between electro-active bacteria and methanogens for substrate can be favored towards electro-active bacteria by controlling at a higher overpotential compared to the thermodynamic equilibrium potential − 0.49 V vs Ag/AgCl [66]. This means that a larger change in granule potential is required, and thus a longer residence time may be preferred for the long-term operation of a moving bed capacitive bioanode. Another factor to influence the capacitive bioanode, is the charging time [16,18,19,30,33,66]. For the moving bed capacitive bioanode, the charging time is the time that the granules are present outside of the discharge cell. Though the charging phase was less efficient for this abiotic study (see Section 3.1), as a capacitive bioanode the charging phase was always long enough for the granules to be fully charged, resulting in a high ΔE, and the charging thus was never seen to limit the bioanode reactor [22].

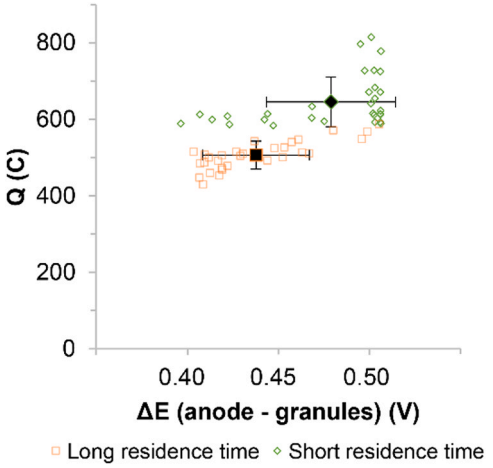

Fig. 5. Charge produced at different granular flowrates (0.6 and 1.7 mm/s).

The beneficial effect of the higher flowrate was also observed in FCDI systems. Similar to the moving bed, the slurry of suspended powder particles forms a flowing capacitive electrode. A “convective current” [55,58] or “hydraulic current” [61,67] was used to describe the effect of charge entering [61] and leaving [55,58,61,67,68] the cell via the capacitive particles. This current increased with increased slurry flow velocity, up to the point the slurry was thinned due to larger shear effects at the highest flowrates [36]. This is unlikely an issue for the moving bed, where the carbon content is 48.6 wt% (for a bulk density of 0.486 g/cm^3) compared to the carbon content of 10–20 wt% [49,56,67] of slurry electrodes. The moving granular bed thus has a denser, and therefore a better connected particle network, and if operated equally (potential, electrolyte conductivity and capacitance), a higher charge density per volume, compared to the carbon slurry.

3.4. The discharge resistance decreased due release of ions in the local electrolyte

The maximum resistance during discharging was calculated from the measured ΔE and the current. The discharge resistance is the maximum as it is calculated from the ΔE, with the potential of the charged granules before discharging in the discharge cell, and the current. Fig. 6A shows the average discharge resistance and the ohmic resistance for each of the experiments. The ohmic resistance was measured at a current of 0 mA, and not during the discharging experiments (Section 2.3). The discharge resistance inside the discharge cell is difficult to determine, as there will be a gradient in ΔE over the discharge cell due to the increased granule potential (over the length, due to the time spent discharging [19]) and due to the ohmic resistance (over the width of the cell). The ΔE inside the discharge will therefore be lower than the maximum ΔE, and therefore the resistance during discharging will be lower than the maximum as well.

For the studied factors: applied ΔE, bulk electrolyte conductivity, the maximum distance between granules and the current collector(s), and residence time in the discharge cell due to the flowrate, the resistance matches the earlier conclusions: the discharging resistance was lowest at the higher ΔE, short residence time, high bulk electrolyte conductivity, and a short distance to the current collectors. The lowest discharge resistances were found for the short discharge experiment (see SI, Section 1.2). As lower discharging resistance means the ΔE inside the discharge cell was closer to the maximum ΔE, this increased the driving force for discharging and therefore increased the transferred charge for the experiment.

The experiments varying the applied ΔE show an average 1.4 times lower discharge resistance when discharged at 0.5 V compared to 0.3 V. This is surprising, as neither the electrical resistance (the ΔE experiments were performed with the 2WE configuration) nor the bulk conductivity were changed (in comparing 0.3 V to 0.5 V). The decrease in resistance by using higher applied ΔE can be the result of an increase in local ionic conductivity by ions released during discharging [69]. Capacitive deionization studies using fixed [70], suspension [65] and fluidized bed [71] capacitive electrodes, have shown that the ions, released from the porosity during discharging, increase the

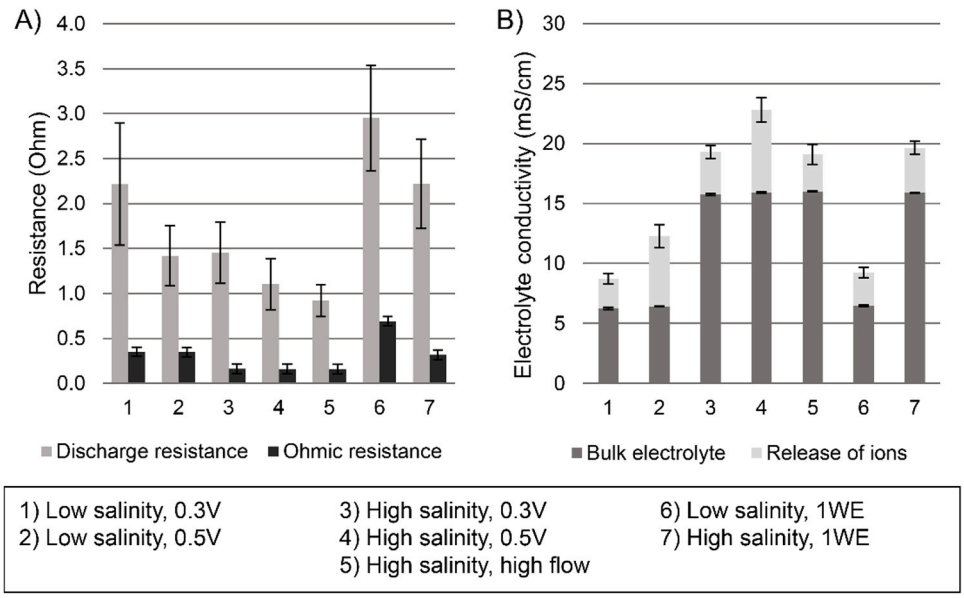

Fig. 6. A) The discharge and ohmic resistance for each of the experiments. The discharge resistance was calculated using the ΔE and current at each measurement interval. The ohmic resistance was measured without ΔE control. B) The measured bulk conductivity and increase in conductivity, calculated from the charge transferred and the residence time, combine to a local increased electrolyte conductivity in the discharge cell. The average and standard deviation over 30 discharge cycles per experiment, are shown for the experiments in Figs. 3–5.

concentrations of ions in the effluent [65,70,71]. It was shown that in the fluidized bed system, the charged capacitive carbon beads carried the ions until they were discharged and increased the ion concentration in the bulk solution [71]. In our study, the discharge step takes place at the current collector(s), thus locally releasing ions in solution in the discharge cell. As more charge is recovered, more ions are released from the pores of the granules [65,70], creating a self-strengthening effect of improving the discharging due to a higher discharge.

At the higher applied ΔE, more charge was harvested from the moving bed. From this charge, we can calculate the concentration of ions released. For instance, the 507 C recovered with the high bulk electrolyte conductivity at 0.5 V would translate to 229 mM of salt released in the discharge cell, compared to 79 mM of salt released for the 175 C in the low bulk electrolyte conductivity experiment at 0.3 V. The bulk conductivity was 6 mS/cm (34 mM) for the low conductivity experiments and 16 mS/cm (115 mM) for the high conductivity experiments. Assuming the electrolyte flow equaled the granular flow, the electrolyte concentration increased in the cell, because of the ions released in the discharge cell. Fig. 6B shows the calculated increase in conductivity, on top of the conductivity of the bulk solution, during each of the experiments. The calculated local conductivity increased to an average of 10 ± 2 mS/cm at low bulk conductivity, 1.6 times increase, and to 20 ± 2 mS/cm at high bulk conductivity, 1.3 times increase compared to the bulk alone. At low bulk electrolyte conductivity, the release of ions lead to a stronger increase in local conductivity than at high bulk electrolyte conductivity. This is due to the non-linear behavior of concentration to conductivity at high concentrations [41].

The discharge resistance was lower for the short residence time experiments, compared to the longer residence time, with a higher discharge current as a result. Interestingly, the increase in local conductivity due to ion release was less for the short discharge time than the long discharge time, indicating that the driving force outweighs the electrolyte conductivity in determining the discharging. The effect of the residence time on the dilution of released ions in the discharge cell is more relevant for the moving bed bioanode reactor, where the driving force is determined by sufficient charging as well.

The release of ions would decrease the ohmic resistance during discharging, but as the discharge process is also influenced by other factors, more study is required to elucidate the self-strengthening effect on the discharging process. This self-strengthening process is especially interesting for BESs, because at low bulk conductivity, such as wastewater conductivity (~1 mS/cm) [72], the local conductivity at the electrode is increased, resulting in lower losses.

For BESs, the effect of the biofilm on the contact resistance and the ion transport resistance (from the porosity) should be investigated. In a previous investigation, the biofilm was not found on the surface but only inside the larger pores [30]. Though this indicates that the biofilm should have limited influence on the contact resistance, older and thus thicker biofilms will increase mass transport limitations [73]. Limitations in mass transport may result in slower release of ions (e.g. protons, sodium, potassium) from the granules into the electrolyte. For the moving bed, this could mean (part of) the ions are released outside of the discharge cell, thus reducing the benefit of the released ions.

4. Conclusions and outlook for application of moving bed reactors

We have studied how four factors influenced the discharging of capacitive granules in a moving granular bed reactor by 1) increasing the potential difference, between the current collector and the granules from 0.3 V to 0.5 V, 2) increasing the bulk electrolyte conductivity from 6 to 16 mS/cm, 3) decreasing the maximum distance between the granules and the current collector by a factor of 2, and 4) decreasing residence time in the discharge cell by a factor of 3.

The largest increase in recovered charge was due to the increase in ΔE. Analysis of the resistance during discharging, with the change in ΔE, indicated the discharging itself increases the charge transfer by an increase in local electrolyte conductivity in the discharge cell. A higher ΔE means both a higher charge recovery and a higher electrode potential. For bioanodes, a high anode potential results in an applied high cell voltage when hydrogen is produced at the cathode [74]. This means there will be an optimum between the recovered charge and the choice of electrode potential, for optimal use of energy recovered from oxidation of organics to produce hydrogen.

Increasing the bulk electrolyte conductivity increased the charge, though less than the ohmic resistance was decreased. The capacitance of the granules, clamped in an external test cell, also increased in higher electrolyte conductivity, and may be the reason behind the higher transferred charge in higher conductivity electrolyte. For bioanodes, the electrolyte conductivity will depend on the choice of wastewater. How the composition of wastewater, as well as the influence of the biofilm, affect the discharging process requires more study.

The transferred charge increased by discharging from both sides of the granular bed. The reduced maximum distance to the current

collector, at the two different bulk electrolytes, showed that the electrical conductivity of the moving bed is more important in determining the transferred charge than the ionic conductivity. Taken together with the increased local electrolyte conductivity, due to the released ions during discharging of the electrons, it can therefore be concluded that, for capacitive bioanodes, improving the electrical conductivity of the moving bed will improve the discharge regardless of the bulk ionic conductivity.

For capacitive bioanodes, the activity in the charging volume is determined by the amount of charge recovered in the discharge cell [30]. For future operation of moving bed bioanodes, we therefore recommend studying the effect of residence time, in the discharge time, on the long-term operation of the bioanode, and to improve the electrical resistance over the granular bed to help to make the driving force more effective in discharging the stored charge in the granules.

CRediT authorship contribution statement

C. Borsje: Conceptualization, Methodology, Investigation, Writing - original draft, Writing - review & editing. **T. Sleutels:** Conceptualization, Methodology, Writing - review & editing. **C.J.N. Buisman:** Conceptualization, Writing - review & editing, Funding acquisition. **A. ter Heijne:** Conceptualization, Methodology, Writing - review & editing.

Declaration of Competing Interest

The authors declare that they have no known competing financial interests or personal relationships that could have appeared to influence the work reported in this paper.

Acknowledgements

This work was performed in the cooperation framework of Wetsus, European Centre of Excellence for Sustainable Water Technology (www.wetsus.nl). Wetsus is co-funded by the Dutch Ministry of Economic Affairs and Ministry of Infrastructure and Environment, the European Union Regional Development Fund, the Province of Fryslân, and the Northern Netherlands Provinces. The authors thank the participants of the research theme “Resource Recovery” for the fruitful discussions and their financial support.

Appendix A. Supporting information

Supplementary data associated with this article can be found in the online version at doi:10.1016/j.jece.2021.105556.

References

[1] M. Qadir, P. Drechsel, B. Jiménez Cisneros, Y. Kim, A. Pramanik, P. Mehta, O. Olaniyan, Global and regional potential of wastewater as a water, nutrient and energy source, Nat. Resour. Forum 44 (2020) 40–51, https://doi.org/10.1111/1477-8947.12187.

[2] D. Puyol, D.J. Batstone, T. Hülsen, S. Astals, M. Peces, J.O. Krömer, Resource recovery from wastewater by biological technologies: opportunities, challenges, and prospects, Front. Microbiol. 7 (2017) 1–23, https://doi.org/10.3389/fmicb.2016.02106.

[3] B.E. Logan, B. Hamelers, R. Rozendal, U. Schröder, J. Keller, S. Freguia, P. Aelterman, W. Verstraete, K. Rabaey, Microbial fuel cells: methodology and technology, Environ. Sci. Technol. 40 (2006) 5181–5192, https://doi.org/10.1021/es0605016.

[4] R.A. Rozendal, H.V.M. Hamelers, G. Euverink, S. Metz, C.J.N. Buisman, Principle and perspectives of hydrogen production through biocatalyzed electrolysis, Int. J. Hydrog. Energy 31 (2006) 1632–1640, https://doi.org/10.1016/j.ijhydene.2005.12.006.

[5] T.H.J.A. Sleutels, H.V.M. Hamelers, C.J.N. Buisman, Reduction of pH buffer requirement in bioelectrochemical systems, Environ. Sci. Technol. 44 (2010) 8259–8263, https://doi.org/10.1021/es101858f.

[6] B.E. Logan, K. Rabaey, Conversion of wastes into bioelectricity and chemicals by using microbial electrochemical technologies, Science 337 (80) (2012) 686–690, https://doi.org/10.1126/science.1217412.

[7] R.A. Rozendal, E. Leone, J. Keller, K. Rabaey, Efficient hydrogen peroxide generation from organic matter in a bioelectrochemical system, Electrochem. Commun. 11 (2009) 1752–1755, https://doi.org/10.1016/j.elecom.2009.07.008.

[8] M. Rodríguez Arredondo, P. Kuntke, A. ter Heijne, C.J.N. Buisman, The concept of load ratio applied to bioelectrochemical systems for ammonia recovery, J. Chem. Technol. Biotechnol. 94 (2019) 2055–2061, https://doi.org/10.1002/jctb.5992.

[9] P. Zamora, T. Georgieva, A. ter Heijne, T.H.J.A. Sleutels, A.W. Jeremiasse, M. Saakes, C.J.N. Buisman, P. Kuntke, Ammonia recovery from urine in a scaled-up microbial electrolysis cell, J. Power Sources 356 (2017) 491–499, https://doi.org/10.1016/j.jpowsour.2017.02.089.

[10] P. Kuntke, T.H.J.A. Sleutels, M. Rodríguez Arredondo, S. Georg, S.G. Barbosa, A. ter Heijne, H.V.M. Hamelers, C.J.N. Buisman, (Bio)electrochemical ammonia recovery: progress and perspectives, Appl. Microbiol. Biotechnol. 102 (2018) 3865–3878, https://doi.org/10.1007/s00253-018-8888-6.

[11] R.D. Cusick, B.E. Logan, Phosphate recovery as struvite within a single chamber microbial electrolysis cell, Bioresour. Technol. 107 (2012) 110–115, https://doi.org/10.1016/j.biortech.2011.12.038.

[12] Y. Lei, M. Du, P. Kuntke, M. Saakes, R. van der Weijden, C.J.N. Buisman, Energy efficient phosphorus recovery by microbial electrolysis cell induced calcium phosphate precipitation, ACS Sustain. Chem. Eng. 7 (2019) 8860–8867, https://doi.org/10.1021/acssuschemeng.9b00867.

[13] S. Chen, G. Liu, R. Zhang, B. Qin, Y. Luo, Development of the microbial electrolysis desalination and chemical-production cell for desalination as well as acid and alkali productions, Environ. Sci. Technol. 46 (2012) 2467–2472, https://doi.org/10.1021/es203332g.

[14] B.E. Logan, M.J. Wallack, K.-Y.Y. Kim, W. He, Y. Feng, P.E. Saikaly, Assessment of microbial fuel cell configurations and power densities, Environ. Sci. Technol. Lett. 2 (2015) 206–214, https://doi.org/10.1021/acs.estlett.5b00180.

[15] A. Deeke, T.H.J.A. Sleutels, T.F.W. Donkers, H.V.M. Hamelers, C.J.N. Buisman, A. ter Heijne, Fluidized capacitive bioanode as a novel reactor concept for the microbial fuel cell, Environ. Sci. Technol. 49 (2015) 1929–1935, https://doi.org/10.1021/es503063n.

[16] A. Deeke, T.H.J.A. Sleutels, H.V.M. Hamelers, C.J.N. Buisman, Capacitive bioanodes enable renewable energy storage in microbial fuel cells, Environ. Sci. Technol. 46 (2012) 3554–3560, https://doi.org/10.1021/es204126r.

[17] A. Deeke, T.H.J.A. Sleutels, A. ter Heijne, H.V.M. Hamelers, C.J.N. Buisman, Influence of the thickness of the capacitive layer on the performance of bioanodes in microbial fuel cells, J. Power Sources 243 (2013) 611–616, https://doi.org/10.1016/j.jpowsour.2013.05.195.

[18] L. Caizán-Juanarena, C. Borsje, T. Sleutels, D. Yntema, C. Santoro, I. Ieropoulos, F. Soavi, A. ter Heijne, Combination of bioelectrochemical systems and electrochemical capacitors: principles, analysis and opportunities, Biotechnol. Adv. 39 (2020), 107456, https://doi.org/10.1016/j.biotechadv.2019.107456.

[19] L. Caizán-Juanarena, I. Servin-Balderas, X. Chen, C.J.N. Buisman, A. ter Heijne, Electrochemical and microbiological characterization of single carbon granules in a multi-anode microbial fuel cell, J. Power Sources 435 (2019), 126514, https://doi.org/10.1016/j.jpowsour.2019.04.042.

[20] S. Porada, R. Zhao, A. van der Wal, V. Presser, P.M. Biesheuvel, Review on the science and technology of water desalination by capacitive deionization, Prog. Mater. Sci. 58 (2013) 1388–1442, https://doi.org/10.1016/j.pmatsci.2013.03.005.

[21] J. Liu, F. Zhang, W. He, X. Zhang, Y. Feng, B.E. Logan, Intermittent contact of fluidized anode particles containing exoelectrogenic biofilms for continuous power generation in microbial fuel cells, J. Power Sources 261 (2014) 278–284, https://doi.org/10.1016/j.jpowsour.2014.03.071.

[22] C. Borsje, T. Sleutels, W. Zhang, W. Feng, C.J.N. Buisman, A. ter Heijne, Making the best use of capacitive current: comparison between fixed and moving granular bioanodes, J. Power Sources 489 (2021), 229453, https://doi.org/10.1016/j.jpowsour.2021.229453.

[23] Y. Liu, X. Sun, D. Yin, L. Cai, L. Zhang, Suspended anode-type microbial fuel cells for enhanced electricity generation, RSC Adv. 10 (2020) 9868–9877, https://doi.org/10.1039/C9RA08288C.

[24] J. Li, Z. Ge, Z. He, A fluidized bed membrane bioelectrochemical reactor for energy-efficient wastewater treatment, Bioresour. Technol. 167 (2014) 310–315, https://doi.org/10.1016/j.biortech.2014.06.034.

[25] S. Tejedor-Sanz, J.M. Ortiz, A. Esteve-Núñez, Merging microbial electrochemical systems with electrocoagulation pretreatment for achieving a complete treatment of brewery wastewater, Chem. Eng. J. 330 (2017) 1068–1074, https://doi.org/10.1016/j.cej.2017.08.049.

[26] J. Li, S. Luo, Z. He, Cathodic fluidized granular activated carbon assisted-membrane bioelectrochemical reactor for wastewater treatment, Sep. Purif. Technol. 169 (2016) 241–246, https://doi.org/10.1016/j.seppur.2016.06.014.

[27] J. Liu, F. Zhang, W. He, W. Yang, Y. Feng, B.E. Logan, A microbial fluidized electrode electrolysis cell (MFEEC) for enhanced hydrogen production, J. Power Sources 271 (2014) 530–533, https://doi.org/10.1016/j.jpowsour.2014.08.042.

[28] Y.U.E. Xuehai, W. Xuyun, Z. Shuju, K. Weifang, G.U.O. Qingjie, W.F. Kong, Q. J. Guo, X.Y. Wang, X.H. Yue, Electricity generation from wastewater using an anaerobic fluidized bed microbial fuel cell, Ind. Eng. Chem. Res. 50 (2011) 12225–12232, https://doi.org/10.1021/ie2007505.

[29] P.T. Ha, H. Moon, B.H. Kim, H.Y. Ng, I.S. Chang, Determination of charge transfer resistance and capacitance of microbial fuel cell through a transient response analysis of cell voltage, Biosens. Bioelectron. 25 (2010) 1629–1634, https://doi.org/10.1016/j.bios.2009.11.023.

[30] C. Borsje, T. Sleutels, M. Saakes, C.J.N. Buisman, A. ter Heijne, The granular capacitive moving bed reactor for the scale up of bioanodes, J. Chem. Technol. Biotechnol. 94 (2019) 2738–2748, https://doi.org/10.1002/jctb.6091.

[31] V.G. Gude, Wastewater treatment in microbial fuel cells – an overview, J. Clean. Prod. 122 (2016) 287–307, https://doi.org/10.1016/j.jclepro.2016.02.022.
[32] C. Borsje, D. Liu, T.H.J.A. Sleutels, C.J.N. Buisman, A. ter Heijne, Performance of single carbon granules as perspective for larger scale capacitive bioanodes, J. Power Sources 325 (2016) 690–696, https://doi.org/10.1016/j.jpowsour.2016.06.092.
[33] F. Soavi, C. Santoro, Supercapacitive operational mode in microbial fuel cell, Curr. Opin. Electrochem. 22 (2020) 1–8, https://doi.org/10.1016/j.coelec.2020.03.009.
[34] B.K. Ferreira, Three-dimensional electrodes for the removal of metals from dilute solutions: a review, Miner. Process. Extr. Metall. Rev. 29 (2008) 330–371, https://doi.org/10.1080/08827500802045586.
[35] V.M. Fischer, In Situ Electrochemical Regeneration of Activated Carbon, s.n., 2001.
[36] C.R. Dennison, M. Beidaghi, K.B. Hatzell, J.W. Campos, Y. Gogotsi, E.C. Kumbur, Effects of flow cell design on charge percolation and storage in the carbon slurry electrodes of electrochemical flow capacitors, J. Power Sources 247 (2014) 489–496, https://doi.org/10.1016/j.jpowsour.2013.08.101.
[37] B. Marinho, M. Ghislandi, E. Tkalya, C.E. Koning, G. de With, Electrical conductivity of compacts of graphene, multi-wall carbon nanotubes, carbon black, and graphite powder, Powder Technol. 221 (2012) 351–358, https://doi.org/10.1016/j.powtec.2012.01.024.
[38] C. Zhong, Y. Deng, W. Hu, J. Qiao, L. Zhang, J. Zhang, A review of electrolyte materials and compositions for electrochemical supercapacitors, Chem. Soc. Rev. 44 (2015) 7484–7539, https://doi.org/10.1039/C5CS00303B.
[39] L. Caizán-Juanarena, T. Sleutels, C. Borsje, A. ter Heijne, Considerations for application of granular activated carbon as capacitive bioanode in bioelectrochemical systems, Renew. Energy 157 (2020) 782–792, https://doi.org/10.1016/j.renene.2020.05.049.
[40] H.A. Andreas, Self-discharge in electrochemical capacitors: a perspective article, J. Electrochem. Soc. 162 (2015) A5047–A5053, https://doi.org/10.1149/2.0081505jes.
[41] Rosemount Analytical, Conductance data for commonly used chemicals, 2010. ⟨https://www.emerson.com/documents/automation/manual-conductance-data-for-commonly-used-chemicals-rosemount-en-68896.pdf⟩. (Accessed January 28 2021).
[42] R.C. Weast, D.R. Lide, Electrical conductivity of aqueous solutions, in: D.R. Lide (Ed.), CRC Handbook of Chemistry and Physics, seventy ed., CRC Press, Boca Raton, 1989, pp. D–221.
[43] H. Cohen, S.E. Eli, M. Jōgi, M.E. Suss, Suspension electrodes combining slurries and upflow fluidized beds, ChemSusChem 9 (2016) 3045–3048, https://doi.org/10.1002/cssc.201601008.
[44] J.W. Campos, M. Beidaghi, K.B. Hatzell, C.R. Dennison, B. Musci, V. Presser, E. C. Kumbur, Y. Gogotsi, Investigation of carbon materials for use as a flowable electrode in electrochemical flow capacitors, Electrochim. Acta 98 (2013) 123–130, https://doi.org/10.1016/j.electacta.2013.03.037.
[45] M. Inagaki, H. Konno, O. Tanaike, Carbon materials for electrochemical capacitors, J. Power Sources 195 (2010) 7880–7903, https://doi.org/10.1016/j.jpowsour.2010.06.036.
[46] J. Schindelin, I. Arganda-Carreras, E. Frise, V. Kaynig, M. Longair, T. Pietzsch, S. Preibisch, C. Rueden, S. Saalfeld, B. Schmid, J.-Y. Tinevez, D.J. White, V. Hartenstein, K. Eliceiri, P. Tomancak, A. Cardona, Fiji: an open-source platform for biological-image analysis, Nat. Methods 9 (2012) 676–682, https://doi.org/10.1038/nmeth.2019.
[47] C.T. Rueden, J. Schindelin, M.C. Hiner, B.E. DeZonia, A.E. Walter, E.T. Arena, K. W. Eliceiri, ImageJ2: ImageJ for the next generation of scientific image data, BMC Bioinform. 18 (2017) 529, https://doi.org/10.1186/s12859-017-1934-z.
[48] R. Zhao, P.M. Biesheuvel, H. Miedema, H. Bruning, A. van der Wal, Charge efficiency: a functional tool to probe the double-layer structure inside of porous electrodes and application in the modeling of capacitive deionization, J. Phys. Chem. Lett. 1 (2010) 205–210, https://doi.org/10.1021/jz900154h.
[49] K.B. Hatzell, M. Boota, Y. Gogotsi, Materials for suspension (semi-solid) electrodes for energy and water technologies, Chem. Soc. Rev. 44 (2015) 8664–8687, https://doi.org/10.1039/C5CS00279F.
[50] S.I. Jeon, H.R. Park, J.G. Yeo, S. Yang, C.H. Cho, M.H. Han, D.K. Kim, Desalination via a new membrane capacitive deionization process utilizing flow-electrodes, Energy Environ. Sci. 6 (2013) 1471–1475, https://doi.org/10.1039/c3ee24443a.
[51] K. Tang, S. Yiacoumi, Y. Li, J. Gabitto, C. Tsouris, Optimal conditions for efficient flow-electrode capacitive deionization, Sep. Purif. Technol. 240 (2020), 116626, https://doi.org/10.1016/j.seppur.2020.116626.
[52] K.B. Hatzell, J. Eller, S.L. Morelly, M.H. Tang, N.J. Alvarez, Y. Gogotsi, Direct observation of active material interactions in flowable electrodes using X-ray tomography, Faraday Discuss. 199 (2017) 511–524, https://doi.org/10.1039/C6FD00243A.
[53] S. Yang, J. Choi, J. Yeo, S. Jeon, H. Park, D.K. Kim, Flow-electrode capacitive deionization using an aqueous electrolyte with a high salt concentration, Environ. Sci. Technol. 50 (2016) 5892–5899, https://doi.org/10.1021/acs.est.5b04640.
[54] A. Rommerskirchen, Y. Gendel, M. Wessling, Single module flow-electrode capacitive deionization for continuous water desalination, Electrochem. Commun. 60 (2015) 34–37, https://doi.org/10.1016/j.elecom.2015.07.018.
[55] A. Rommerskirchen, A. Kalde, C.J. Linnartz, L. Bongers, G. Linz, M. Wessling, Unraveling charge transport in carbon flow-electrodes: performance prediction for desalination applications, Carbon 145 (2019) 507–520, https://doi.org/10.1016/j.carbon.2019.01.053.
[56] S. Porada, D. Weingarth, H.V.M. Hamelers, M. Bryjak, V. Presser, P.M. Biesheuvel, Carbon flow electrodes for continuous operation of capacitive deionization and capacitive mixing energy generation, J. Mater. Chem. A 2 (24) (2014) 9313, https://doi.org/10.1039/c4ta01783h.
[57] S. Porada, J. Lee, D. Weingarth, V. Presser, Continuous operation of an electrochemical flow capacitor, Electrochem. Commun. 48 (2014) 178–181, https://doi.org/10.1016/j.elecom.2014.08.023.
[58] N.C. Hoyt, E. Agar, E.A. Nagelli, R. Savinell, J. Wainright, Electrochemical impedance spectroscopy of flowing electrosorptive slurry electrodes, J. Electrochem. Soc. 165 (2018) E439–E444, https://doi.org/10.1149/2.0051810jes.
[59] M. Boota, K.B. Hatzell, M. Beidaghi, C.R. Dennison, E.C. Kumbur, Y. Gogotsi, Activated carbon spheres as a flowable electrode in electrochemical flow capacitors, J. Electrochem. Soc. 161 (2014) A1078–A1083, https://doi.org/10.1149/2.072406jes.
[60] M. Boota, K.B. Hatzell, M. Alhabeb, E.C. Kumbur, Y. Gogotsi, Graphene-containing flowable electrodes for capacitive energy storage, Carbon 92 (2015) 142–149, https://doi.org/10.1016/j.carbon.2015.04.020.
[61] C.R. Dennison, Y. Gogotsi, E.C. Kumbur, In situ distributed diagnostics of flowable electrode systems: resolving spatial and temporal limitations, Phys. Chem. Chem. Phys. 16 (2014) 18241–18252, https://doi.org/10.1039/C4CP02820A.
[62] F. Liu, O. Coronell, D.F. Call, Electricity generation using continuously recirculated flow electrodes in reverse electrodialysis, J. Power Sources 355 (2017) 206–210, https://doi.org/10.1016/j.jpowsour.2017.04.061.
[63] C. Zhang, K.B. Hatzell, M. Boota, B. Dyatkin, M. Beidaghi, D. Long, W. Qiao, E. C. Kumbur, Y. Gogotsi, Highly porous carbon spheres for electrochemical capacitors and capacitive flowable suspension electrodes, Carbon 77 (2014) 155–164, https://doi.org/10.1016/j.carbon.2014.05.017.
[64] R. Gloukhovski, M.E. Suss, Measurements of the electric conductivity of MWCNT suspension electrodes with varying potassium bromide electrolyte ionic strength, J. Electrochem. Soc. 167 (2020), 020528, https://doi.org/10.1149/1945-7111/ab6a88.
[65] J. Ma, P. Liang, X. Sun, H. Zhang, Y. Bian, F. Yang, J. Bai, Q. Gong, X. Huang, Energy recovery from the flow-electrode capacitive deionization, J. Power Sources 421 (2019) 50–55, https://doi.org/10.1016/j.jpowsour.2019.02.082.
[66] C. Santoro, F. Soavi, A. Serov, C. Arbizzani, P. Atanassov, Self-powered supercapacitive microbial fuel cell: the ultimate way of boosting and harvesting power, Biosens. Bioelectron. 78 (2016) 229–235, https://doi.org/10.1016/j.bios.2015.11.026.
[67] T.J. Petek, N.C. Hoyt, R.F. Savinell, J.S. Wainright, Characterizing slurry electrodes using electrochemical impedance spectroscopy, J. Electrochem. Soc. 163 (2016) A5001–A5009, https://doi.org/10.1149/2.0011601jes.
[68] N.C. Hoyt, R.F. Savinell, J.S. Wainright, Modeling of flowable slurry electrodes with combined faradaic and nonfaradaic currents, Chem. Eng. Sci. 144 (2016) 288–297, https://doi.org/10.1016/j.ces.2016.01.048.
[69] J. Kang, T. Kim, H. Shin, J. Lee, J.I. Ha, J. Yoon, Direct energy recovery system for membrane capacitive deionization, Desalination 398 (2016) 144–150, https://doi.org/10.1016/j.desal.2016.07.025.
[70] L. Wang, P.M. Biesheuvel, S. Lin, Reversible thermodynamic cycle analysis for capacitive deionization with modified Donnan model, J. Colloid Interface Sci. 512 (2018) 522–528, https://doi.org/10.1016/j.jcis.2017.10.060.
[71] G.J. Doornbusch, J.E. Dykstra, P.M. Biesheuvel, M.E. Suss, Fluidized bed electrodes with high carbon loading for water desalination by capacitive deionization, J. Mater. Chem. A 4 (2016) 3642–3647, https://doi.org/10.1039/C5TA10316A.
[72] R.A. Rozendal, H.V.M. Hamelers, K. Rabaey, J. Keller, C.J.N. Buisman, Towards practical implementation of bioelectrochemical wastewater treatment, Trends Biotechnol. 26 (2008) 450–459, https://doi.org/10.1016/j.tibtech.2008.04.008.
[73] A.C.L. de Lichtervelde, A. ter Heijne, H.V.M. Hamelers, P.M. Biesheuvel, J. E. Dykstra, Theory of ion and electron transport coupled with biochemical conversions in an electroactive biofilm, Phys. Rev. Appl. 12 (2019), 014018, https://doi.org/10.1103/PhysRevApplied.12.014018.
[74] T.H.J.A. Sleutels, A. ter Heijne, C.J.N. Buisman, H.V.M. Hamelers, Bioelectrochemical systems: an outlook for practical applications, ChemSusChem 5 (2012) 1012–1019, https://doi.org/10.1002/cssc.201100732.